Volume 22, No 3 | International Journal of Radiation Research, July 2024

Impact of diffusion kurtosis imaging as an early prognostic factor following radiotherapy in patients with head and neck squamous cell carcinoma

T. Itonaga[1*], R. Mikami[1], T. Zama[1], Y. Okada[1], M. Kurooka[1], Y. Araki[1], M. Okubo[2], S. Sugahara[3], K. Saito[1]

[1]*Department of Radiology, Tokyo Medical University Hospital, 6-7-1 Nishi-shinjyuku,Shinjyuku, Tokyo, Japan*
[2]*Departments of Radiology, Tokyo Medical University Hachioji Medical Center, 1163 Tate-machi, Hachioji, Tokyo, Japan*
[3]*Departments of Radiology, Tokyo Medical University Ibaraki Medical Center, 3-20-1 Chuo, Ami-machi, Inashiki-gun, Ibaraki, Japan*

► ***Original article***

Corresponding author:
Tomohiro Itonaga M.D., Ph.D.,
E-mail:
itonaga@tokyo-med.ac.jp

Received: September 2023
Final revised: March 2024
Accepted: March 2024

Int. J. Radiat. Res., July 2024; 22(3): 603-608

DOI: 10.61186/ijrr.22.3.603

Keywords: *Cancer of head and neck, biomarkers, radiotherapy, diffusion magnetic resonance imaging.*

ABSTRACT

Background: Radiotherapy has an essential position in the definitive therapy of head and neck squamous cell carcinoma (HNSCC); however, imaging markers with prognostic value are unknown. Here, we determined whether diffusion kurtosis imaging (DKI) derived from magnetic resonance imaging (MRI) before radiotherapy in patients with HNSCC could be useful as outcome predictor for early treatment response. ***Material and Methods:*** Thirty-six patients with 86 lesions who underwent definitive radiotherapy for HNSCC were enrolled. The standardized uptake value (SUV) max and mean, metabolic tumor volume (MTV), total lesion glycolysis (TLG) from positron emission tomography-computed tomography (PET-CT), tumor diameter from CT images, and mean kurtosis (MK) values of DKI from MRI were compared as imaging biomarkers to predict an early response following radiotherapy. A total dose of 70 Gy was administered for all lesions. To determine whether DKI derived from MRI before radiotherapy in patients with HNSCC is useful as a prognostic predictor of early treatment response, patient response was assessed via endoscopy and imaging studies three months after treatment. ***Results:*** Correlation between MK mean and SUV max, TGL, MTV, and tumor diameter was not observed; however, significant differences in the imaging parameters were observed for overall response rate (ORR) (CR + PR) for MK mean and TLG; ORR group having significantly higher MK means than the non-ORR group. The MK values significantly correlated with the ORR of radiotherapy. ***Conclusion:*** DKI parameters that are measured quantitatively within a short imaging time can be prognostic factors before radiotherapy.

INTRODUCTION

Form- and function-sparing chemoradiation or radiation alone are used in patients with head and neck squamous cell carcinoma (HNSCC) at various disease stages [1,2]. Recent technological advances have enabled precise delivery of higher prescribed doses to targeted lesions and lower doses to the surrounding normal tissue. However, radiotherapy delivers the same dose to the target regardless of tumor molecular characteristics and has limited breakthroughs in treating individual patients. Therefore, "Precision Medicine," which considers biomarkers and general medical information to establish a patient's genetic background and disease status to curate individualized treatment, has garnered attention [3]. Biomarkers, including genes, proteins, peptides, and images, are defined as quantitatively measured and evaluated as markers of therapeutic effects or biological or pathogenic processes [4].

With recent advancements in diagnostic imaging, imaging biomarkers have become increasingly popular for visualizing tumor dynamics, predicting treatment efficacy, and prognosis. Current imaging biomarkers for HNSCC include tumor diameter, extranodal extension, and central necrosis using computed tomography (CT) images [5-7]. Although CT images offer high-resolution and macroscopic blood flow information, they lack functional information, such as tumor activity. Pre-treatment ^{18}F-fluoro-2-deoxyglucose positron emission tomography-computed tomography (FDG PET-CT) is commonly utilized in nuclear medicine as an imaging tool, but it involves radiation exposure and has lower resolution than CT [8,9]. In contrast, magnetic resonance imaging (MRI) offers functional information of tissues and comprehensive understanding of complex head and neck (H&N) structures without radiation exposure. Diffusion-weighted imaging (DWI) is a parameter which visualizes the movement of water molecules within tissues. A prospective study has reported DWI

[DOI: 10.61186/ijrr.22.3.603]

was valuable predictive factor of treatment outcome in H&N cancer patients [10].

DWI is limited to free diffusion within a normal distribution in homogeneous and broad fluids. This makes it challenging to accurately observe complex biological information. Methods, such as q space imaging (QSI) and diffusion kurtosis imaging (DKI), which measure the diffusion of water molecules based on a non-Gaussian distribution, can overcome this problem [11,12]. QSI is an imaging method that exploits the dynamics of microscopic water molecules at the micrometer level. A probability density function for each motion probing gradient (MPG) by Fourier transforming the DWI signal attenuation curves is obtained from data captured with a large number of b-values. As this method requires the application of many b-values and MPGs in multiple axes, it has the disadvantage of prolonging the imaging time and increasing analysis complexity. DKI is an imaging method that specializes only in kurtosis, a quantitative value that represents the difference from the normal distribution measurable by QSI. Unlike QSI, DKI requires a minimum of three b -values, making it better for clinical use. Previous studies have suggested that DKI was a useful predictive factor for various cancers, including H&N cancer [13-15]. Therefore, we determined whether DKI obtained from pre-treatment MRI images of patients with HNSCC is a useful prognostic factor for early treatment response compared with conventional imaging biomarkers. To our knowledge, this is the first report to compare PET parameters against DKI as an imaging biomarker before radiotherapy in HNSCC patients.

MATERIALS AND METHODS

Patients

Patients who underwent radiotherapy against HNSCC at Tokyo Medical University Hospital between January 2020 and November 2021 were included in this study (IRB number: T2022-0081, Date of registration: July 29th, 2022), which was approved by the our hospital ethics committee, and informed consent was obtained as an opt-out. All patients also signed written consent for the using of imaging data from their examination at the hospital. The eligibility criteria: 1) age ≥20 years; 2) no history of radiotherapy to the H&N; 3) diagnosis of squamous cell carcinoma by cytology or histology; 4) MRI performed within one month and PET-CT within six months before the start of radiotherapy; and 5) post-treatment examination at our institution within six months after the completion of radiotherapy. Thirty-six patients (median age: 63 years, female:male = 5:31) with 86 lesions met the eligibility criteria. Table 1 lists the patient and tumor characteristics. Eclipse (Varian Medical Systems, Palo Alto, CA, USA) was used as the radiation therapy planning system and a total of 70 Gy was prescribed at 2 Gy per day for all target lesions. The irradiation technique involved the use of intensity-modulated or 3D conformal radiation therapy with the TrueBeam, a linear accelerator from Varian Medical Systems (Palo Alto, CA, USA).

Table 1. Patient and tumor characteristics.

No	Age	Sex	Measurement lesion	Primary tumor	Treatment	T factor of TNM 8th	Day to MRI and start of RT
1	47	M	P*,N#	Oro p16+	CCRT	2	**21**
2	71	M	P	Oro p16+	CCRT	2	6
3	57	M	P,N	Oro p16+	CCRT	2	5
4	56	M	P	Larynx	CCRT	3	12
5	35	M	P,N	Naso	CCRT	4	9
6	64	M	P,N	Naso	CCRT	3	14
7	65	M	P	Oro p16+	CCRT	1	12
8	74	M	P	Larynx	CCRT	3	7
9	50	M	P,N	Hypo	CCRT	2	12
10	76	M	P,N	Oro p16-	RT	1	11
11	73	F	P	Maxillary	CCRT	4a	15
12	44	M	P	Maxillary	CCRT	3	12
13	68	M	P	Oro p16- (R)	CCRT	N/A	8
14	72	M	P,N	Oro p16-	CCRT	4b	1
15	63	M	P,N	Hypo	CCRT	2	8
16	67	F	P	Naso	CCRT	3	5
17	61	M	P,N	Hypo	CCRT	2	5
18	48	M	P	Hypo	CCRT	4a	8
19	58	M	P	Hypo	CCRT	2	7
20	70	M	P,N	Oro p16-	CCRT	4a	13
21	83	F	P,N	Oro p16+	RT	2	6
22	62	M	P,N	Oro p16+	CCRT	2	7
23	50	F	P,N	Oro p16+	CCRT	2	1
24	59	M	P,N	Naso	CCRT	4	22
25	75	M	P	Hypo	CCRT	2	1
26	74	M	P	Hypo	RT	2	7
27	50	M	P	Oro p16+	CCRT	2	13
28	52	F	P,N	Hypo	CCRT	4a	8
29	69	M	P,N	Oro p16-	CCRT	4a	8
30	60	M	N	Larynx	CCRT	4a	12
31	50	M	N	Oro p16+ (R)$	CCRT	N/A	12
32	47	M	P,N	Larynx	CCRT	2	14
33	38	M	P,N	Naso	CCRT	1	1
34	77	M	P,N	Oral (R)	CCRT	N/A	1
35	66	F	N	Unknown	CCRT	N/A	1
36	74	M	P	Hypo	RT	2	10

Abbreviations: P*, primary/local recurrence; N#, lymph node; Oro p16+, p16+ oropharyngeal cancer; Oro p16−, p16− oropharyngeal cancer; Hypo, hypopharyngeal cancer; Naso, nasopharyngeal cancer; (R)$, recurrence case; N/A, not applicable.

MRI protocol and DKI analysis

All patients underwent Magnetom Vida 3.0 Tesla MRI scanner (Siemens Healthineers, Erlangen, Germany) with a 20 - channel H&N array coil in the supine position one month before radiotherapy. The imaging range extended from the skull base to the clavicle fossa. MR parameters were obtained using a single-shot spin echo EPI sequence with a short inversion time recovery technique, and the following parameters: TR/TE = 5430/68 ms; TI = 230 ms; field of view = 280 × 210 mm^2; voxel size = 0.7 × 0.7 × 5 mm^3; slice thickness = 5 mm; gap = 1 mm; number of

[DOI: 10.61186/ijrr.22.3.603]

slices = 30; diffusion gradient pulse duration (δ) = 14 ms; diffusion gradient separation (Δ) = 34.3 ms; diffusion directions = 3; b-values = 0, 800, and 1500 s/mm^2; scanning time = 3 min 26 s. We defined the region of interest (ROI) as the area surrounded by tumor contour on b = 0 image, referencing the fat-suppressed T2-weighted image. For DKI, at least three b-values are required, and high (500 – 1000) and ultrahigh (1500–2000) values are needed to quantify kurtosis by capturing non-Gaussian diffusion behavior [16,17]. Therefore, b = 800 and 1500 were selected. Mean kurtosis (MK) maps were generated from three b-value image data [18]. MK maps were generated voxel-by-voxel from the three b-value image data using the MATLAB environment software (http://www.mathworks.com) based on equation 1 as follows [19]:

$$S = S_0 \exp\left(-bD + \frac{1}{6}b^2D^2K\right) \quad (1)$$

The "S_0" is the signal intensity at a b-values = 0 s/mm^2 whereas "b" represents the diffuse sensitivity value. While "D" denotes the apparent diffusion coefficient, and "K" denotes the apparent kurtosis coefficient. This software calculates these values to generate an MK map, which represents the average kurtosis of all possible diffusion directions. We used ImageJ (version 1.53) software (U.S. National Institutes of Health, Bethesda, Maryland) to analyze MK values. The MK value is a statistical measure that indicates the extent to which restricted diffusion deviates from normal distribution, and ranges from 0 to 3. All ROIs with a diameter >10 mm were outlined on diffusion-weighted MR images and automatically copied and pasted by the software to the same coordinates on the diffusion kurtosis images (figure 1). A contrast agent was not used in the study.

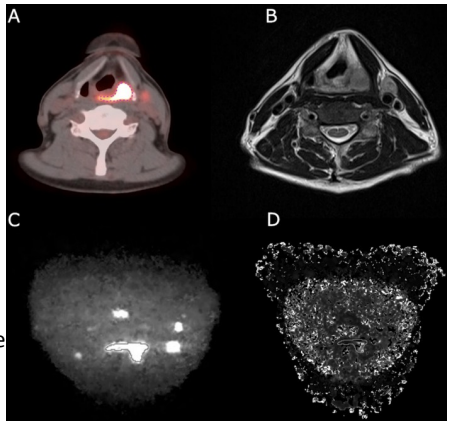

Figure 1. Pre-treatment axial PET-CT and MR images of the primary site of a 61-year-old man with hypopharyngeal cancer. **A)** PET-CT image, **B)** T2-weighted image, **C)** DWI b-values = 1500 s/mm2. **D)** Mean kurtosis map. Images **A–D** are all axial images at the same level, whereas images **C)** and **D)** are mirrored horizontally and vertically for image processing. The region of interest (ROI) of the target tumor area drawn with b = 1500 s/mm2 referring to PET-CT or MRI is registered using ROI Manager of ImageJ. The registered ROI and "Mean kurtosis map" were selected to measure the ROI with the same coordinates. CT, computed tomography; MRI, magnetic resonance imaging; PET, positron emission tomography.

FDG-PET/CT imaging and parameters analysis

All cases underwent PET/CT scans using the Discovery MI PET-CT system (GE Healthcare, Milwaukee, WI, USA) in the supine position 60 min after intravenous injection of 3 – 4 MBq/kg of FDG (FDGscan, Universal Giken, Nihon Mediphysics, Tokyo, Japan). Before the routine PET/CT scans, fasting for at least 6 h and rest in a dimly lit room for at least 40 – 60 min were administered to all patients.

The CT scanning covered the parietal to the diaphragm, with the following imaging parameters: 120 kV, tube current with auto exposure control, scan slice thickness 3.75 mm, and matrix 192 × 192. After applying attenuation correction to the CT images, reconstructed PET images were obtained. For PET parameter analysis, ROI were delineated utilizing PET EdgeTM, which is a semi-automatically gradient-based PET segmentation mechanism in MIM maestro (v. 6.1) software (MIM Software Inc., Cleveland, USA). This mechanism places the contour delineation at a location of the highest signal gradient, and, previously, has been shown to correspond more favorably to pathological tissues than threshold-based mechanisms (20). The max and mean standardized uptake value (SUV), metabolic tumor volume (MTV), and total lesion glycolysis (TLG) were automatically calculated when contouring the target using MIM maestro. TLG was determined by equation 2 as follows:

$$TLG = (MTV) \times (SUV\ mean) \quad (2)$$

Statistical validation

The ROI setting and tumor parameter evaluating were conducted by two radiologists (T.I. 12 years of experience and T.Z., with 11 years). For tumor size, the primary lesion was measured using its maximum diameter, whereas the lymph nodes were measured using the maximum short-axis diameter. Post-treatment evaluation was classified as CR, PR, SD, or PD by endoscopic and imaging findings according to RECIST (v. 1.1) (21). The overall response rate (ORR) was defined as the sum of the percentages of cases showing a CR and PR, with the number of cases treated as the denominator. The Shapiro–Wilk test was applied to evaluate whether continuous variables obey a normal distribution. For those that did not follow a normal distribution, the Mann-Whitney U test was used for the comparison group of subjects, and Spearman's rank correlation was used to determine the correlation between the two groups. Statistically significant difference between the two groups was set at p-value < 0.05. To calculate cutoff values for prognostic analysis, receiver operating characteristic (ROC) curve was created and suitable cutoff values were calculated based on the Youden index and area under the curve (AUC). Statistical analysis of all data was conducted utilizing R (v. 3.1.0) software (R Foundation for Statistical Computing, Vienna, Austria).

[DOI: 10.61186/ijrr.22.3.603]

RESULTS

The median interval from start of radiotherapy to MRI and PET-CT was 8 (range: 1 – 22) and 33 days (range: 6 – 132), respectively. The median interval from the end of radiotherapy to the initial post-treatment evaluation date was 46 days (range: 27 – 78). The median tumor diameter was 20.5 mm (range: 10 – 57 mm). Median tumor parameters for PET and DKI are listed in table 2 for primary and lymph node metastasis (LNm). With respect to tumor parameters, only MK mean did not differ significantly among primary and LNm (p = 0.11). We examined the correlation between the tumor parameters (figure 2). The MK mean did not show a correlation with SUVmax, TGL, MTV, and tumor diameter. At the initial post-treatment evaluation, 55 lesions were categorized as CR, 8 as PR, 22 as SD, and 1 as PD (figure 3). The ORR was 73.3%, and according to the site, 87.9% for primary and 63.0% for LNm. At one year post-treatment, 8 patients (22.9%) experienced recurrence or distant metastasis, with the lung being the most common organ affected. The imaging parameters that showed significant differences for ORR were MK mean (p = 0.02) and TLG (p = 0.049). We individually examined MK mean as a prognostic factor of ORR for primary and LNm; nonetheless, the difference was not significant (Primary: p = 0.08, LNm: p = 0.16). To determine the effect of MK mean and TLG on ORR, ROC curves were analyzed. The optimal cutoff values associated with the AUC and ORR were 0.65 and 0.43 for MK mean and 0.60 and 74.3 for TLG, respectively (figure 4). The analysis of ORR revealed a statistically significant difference when MK mean was stratified with a cutoff value of 0.43 (p = 0.03). In contrast, TLG was stratified with a cutoff value of 74.3; however, there showed no difference that was statistically significant (p = 0.05).

Table 2. Tumor characteristics.

		Size (mm)	SUV max	SUV mean	MTV	TLG	MK Mean
Total	Median (IQR*)	20.5 (15.0-28.0)	15.1 (11.3-18.7)	8.8 (6.0-10.6)	3.5 (1.1-8.8)	30.6 (10.0-85.5)	0.3 (0.2-0.6)
Primary		17.1 (14.1-19.9)	17.1 (14.1-20.0)	9.5 (7.9-11.7)	6.6 (3.7-16.7)	57.4 (30.5-145.5)	0.7 (0.3-1.2)
LNm		13.9 (10.0-17.1)	13.9 (10.0-17.1)	7.9 (5.8-10.2)	1.9 (0.6-5.7)	18.3 (6.9-48.6)	0.3 (0.2-0.5)

Abbreviations: IQR*, Interquartile range: LNm,Lymph node metastasis.

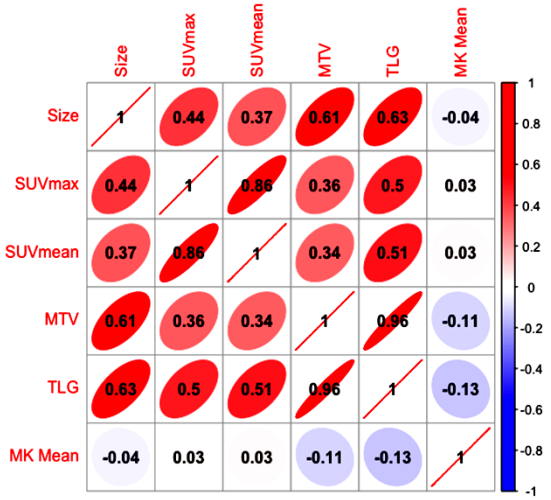

Figure 2. Correlation heat map and scatter matrix. The correlation analysis of tumor diameter, PET parameter, and MK mean is plotted. Scatter plots and colored blocks are used to represent specific correlations and correlation coefficients, respectively. Very low correlations between MK mean and other parameters are shown. PET, positron emission tomography; MK, mean kurtosis.

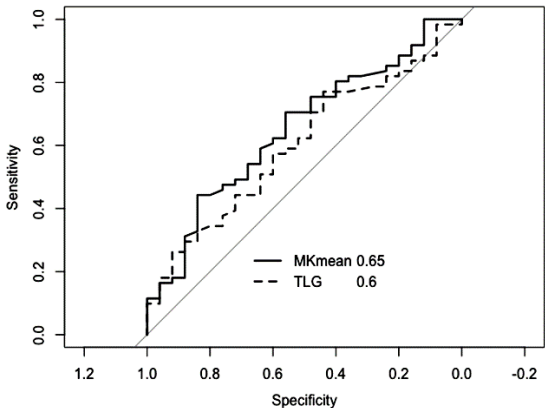

Figure 4. ROC analysis of the MK mean and TLG for ORR after radiotherapy. The solid line represents MK mean and the dotted line represents TLG, and their respective AUCs are listed. ROC, receiver operating characteristic; AUC, area under the curve; MK, mean kurtosis; TLG, total lesion glycolysis.

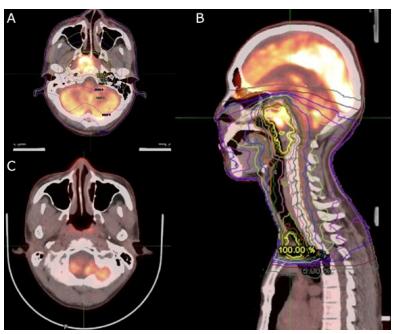

Figure 3. A case of concomitant chemoradiotherapy for nasopharyngeal cancer in a 35-year-old male. Radiotherapy involved a two-step method using an intensity-modulated radiation therapy technique in which 46 Gy/23 fractions were administered to the whole neck, followed by boosting with 24 Gy/12 fractions to the FDG-uptake area. The axial image of the fusion of the treatment plan and PET-CT is shown in **A)** and the sagittal image in **B)** indicating high-dose conformity in the FDG-uptake area. The PET-CT image six months after concomitant chemoradiotherapy is shown in **C)** and the FDG-uptake observed before treatment disappeared, which together with the endoscopic findings led to the evaluation of a complete response. PET-CT, positron emission tomography-computed tomography; FDG, 18F-fluoro-2-deoxyglucose.

[DOI: 10.61186/ijrr.22.3.603]

DISSCUTION

Early prognosis of patients with HNSCC with poor response to radiotherapy is crucial, enabling appropriate patient-specific treatment, such as neck dissection before or after radiotherapy or chemotherapy administation. PET parameters and tumor size are considered predictors of radiotherapy in patients with HNSCC [22,23]. A meta-analysis of H&N cancer patients reported that MTV and TLG from pre-treatment PET/CT are predictors for overall survival (OS) [22]. In this study, as a PET parameter, TLG was a significant predictor of early prognosis after radiotherapy. The median values of MTV and TLG in this study 3.5 and 30.6, respectively, which are lower than the cutoff values of 7.7 – 45 and 55 – 330, respectively, in the meta-analysis, and may have influenced the analysis. This may result from the fact that the present study included locally advanced H&N cancers that could be cured by radiotherapy, whereas the meta-analysis included all H&N cancer patients before therapy. One study on prognostic factors derived from FDG PET-CT before and within radiotherapy against H&N cancer patients indicated that high TLG for the primary tumor predicted poorly for OS and PFS [24]. In this study, TLG of the primary lesions showed no significant prognosis factor, which may have occurred because the PET parameters yield semi-quantitative values [25,26].

With advancemen in MRI technologies, reports on the efficienty of pre-treatment diffusion parameters to predict radiotherapy response in patients with H & N cancer have emerged. Zhang *et al*. described lower local recurrence-free and disease-free survival rates in patients with nasopharyngeal carcinoma have high apparent diffusion coefficient (ADC) values before radiotherapy [27]. However, there are reports of no significant differences in pre-treatment ADC values between responders and non-responders in stage III–IV nasopharyngeal carcinoma following neoadjuvant chemotherapy, making the utility of ADC values is controversial [28]. Conventional ADC values assume Gaussian water diffusion, applicable only when water diffuses freely in a uniform and sufficiently wide fluid; however, have limited applicability when measuring complex *in vivo* structures [29,30]. In this study, we used DKI as an index that can quantitatively evaluate and reflect non -Gaussian distribution. Although QSI is an alternative imaging method for non-Gaussian distribution, DKI proved to be easy to implement in routine clinical use with lesser acquisition time than that of QSI.

We found no correlation between DKI and PET parameters or tumor diameter, which is consistent with previous studies on oral squamous cell carcinoma [31]. This lack of correlation may result from the fact that FDG-PET parameters evaluate tumor tissue metabolism, whereas DKI parameters consider tumor tissue structure based on the water molecules diffusion. The differences in tumor characteristics reflected by DKI parameters may affect the low correlation. Previous studies have indicated that MK increases in tumors with complex tissue structure, reflecting increased cell density and size [12, 32]. Our study suggest lower MK values are related to less effective radiotherapy, possibly, due to increased permeability and disruption of cell membranes in hypoxic regions within the tumor. Previous investigations have indicated a significantly negative relationships between DKI and hypoxic PET tracers, such as ^{18}F-fluoroazomycin arabinoside and ^{18}F-fluoromisonidazole in H&N cancer [31, 33], which supports our hypothesis that MK values may reflect structural changes in hypoxic cells.

This study has several limitations. In the first, although HNSCC patients were included, 34.3% of the patients presented with virus-associated tumors, such as HPV/p16 positive-associated oropharyngeal and EBV-associated nasopharyngeal carcinomas. Second, there were six cases in which the interval from PET-CT to MRI was longer as cervical dissection was performed after PET-CT scanning. Therefore, in these cases, the PET parameters may not accurately reflect tumor information compared to the MRI parameters that were taken immediately before radiotherapy. Finally, this is a retrospective study of early post-treatment prognosis in a small groups. Future prospective studies are needed with a larger number of patients over a longer period.

CONCLUSION

MK values were significantly correlated with the ORR of radiotherapy. DKI parameters that can be quantitatively measured and have a short imaging time may be prognostic factors before radiotherapy.

ACKNOWLEDGEMENT

We would like to thank Dr. Manabu Inagaki of EURO MEDITECH CO., LTD. for technical support regarding MIM Maestro. I would like to express my gratitude to Dr. Daisuke Yoshimaru for providing guidance on DKI analysis.

Funding: This work was supported in part by Bayer Academic support (No. BASJ20210402003).

Conflicts of interests: The authors declare that they have no conflicts of interest.

Ethical consideration: The ethical committee of Tokyo Medical University Hospital approved the study (IRB number. T2022-0081). The study was retrospective and informed consent was provided in the form of an opt-out on the university website.

Author contributions: T.I. and K.S. designed the study. Z.T. performed the data collection and Y.A. and M.K. and R.M. performed the data analysis. S.S. and M.O. were responsible for the statistical analysis, and T.I. wrote the manuscript with the support of Y.O. K.S.

[DOI: 10.61186/ijrr.22.3.603]

supervised this study. All authors approved the final version of the manuscript for publication.

REFERENCES

1. Brizel DM, Albers ME, Fisher SR (1998) Hyperfractionated irradiation with or without concurrent chemotherapy for locally advanced head and neck cancer. *The New England journal of medicine,* ***338(25):*** *1798-1804.*
2. Delaney G, Jacob S, Featherstone C (2005) The role of radiotherapy in cancer treatment: estimating optimal utilization from a review of evidence-based clinical guidelines. *Cancer,* ***104(6):*** *1129-1137.*
3. Tinhofer I, Niehr F, Konschak R (2015) Next-generation sequencing: hype and hope for development of personalized radiation therapy? *Radiat Oncol,* ***10:*** *183.*
4. Biomarkers Definitions Working G (2001) Biomarkers and surrogate endpoints: preferred definitions and conceptual framework. *Clin Pharmacol Ther,* ***69(3):*** *89-95.*
5. Cooper JS, Pajak TF, Forastiere AA (2004) Postoperative concurrent radiotherapy and chemotherapy for high-risk squamous-cell carcinoma of the head and neck. *The New England journal of medicine,* ***350(19):*** *1937-1944.*
6. Knegjens JL, Hauptmann M, Pameijer FA (2011) Tumor volume as prognostic factor in chemoradiation for advanced head and neck cancer. *Head & neck,* ***33(3):*** *375-382.*
7. Zoumalan RA, Kleinberger AJ, Morris LG (2010) Lymph node central necrosis on computed tomography as predictor of extracapsular spread in metastatic head and neck squamous cell carcinoma: pilot study. *J Laryngol Otol,* ***124(12):*** *1284-1288.*
8. Imsande HM, Davison JM, Truong MT (2011) Use of 18F-FDG PET/CT as a predictive biomarker of outcome in patients with head-and-neck non-squamous cell carcinoma. *AJR Am J Roentgenol,* ***197(4):*** *976-980.*
9. Machtay M, Natwa M, Andrel J (2009) Pretreatment FDG-PET standardized uptake value as a prognostic factor for outcome in head and neck cancer. *Head & neck,* ***31(2):*** *195-201.*
10. Ai QY, King AD, Law BK (2017) Diffusion-weighted imaging of nasopharyngeal carcinoma to predict distant metastases. *Eur Arch Otorhinolaryngol,* ***274(2):*** *1045-1051.*
11. Assaf Y, Kafri M, Shinar H (2002) Changes in axonal morphology in experimental autoimmune neuritis as studied by high b-value q-space (1)H and (2)H DQF diffusion magnetic resonance spectroscopy. *Magn Reson Med,* ***48(1):*** *71-81.*
12. Jensen JH, Helpern JA, Ramani A (2005) Diffusional kurtosis imaging: the quantification of non-gaussian water diffusion by means of magnetic resonance imaging. *Magn Reson Med,* ***53(6):*** *1432-1440.*
13. Chen Y, Ren W, Zheng D (2015) Diffusion kurtosis imaging predicts neoadjuvant chemotherapy responses within 4 days in advanced nasopharyngeal carcinoma patients. *J Magn Reson Imaging,* ***42(5):*** *1354-1361.*
14. Kang HS, Kim JY, Kim JJ (2022) Diffusion Kurtosis MR Imaging of Invasive Breast Cancer: Correlations With Prognostic Factors and Molecular Subtypes. *J Magn Reson Imaging,* ***56(1):*** *110-120.*
15. Zhu L, Pan Z, Ma Q (2017) Diffusion Kurtosis Imaging Study of Rectal Adenocarcinoma Associated with Histopathologic Prognostic Factors: *Preliminary Findings. Radiology,* ***284(1):*** *66-76.*
16. Jensen JH, Helpern JA (2010) MRI quantification of non-Gaussian water diffusion by kurtosis analysis. *NMR Biomed,* ***23(7):*** *698-710.*
17. Rosenkrantz AB, Padhani AR, Chenevert TL (2015) Body diffusion kurtosis imaging: Basic principles, applications, and considerations for clinical practice. *J Magn Reson Imaging,* ***42(5):*** *1190-1202.*
18. Tabesh A, Jensen JH, Ardekani BA (2011) Estimation of tensors and tensor-derived measures in diffusional kurtosis imaging. *Magn Reson Med,* ***65(3):*** *823-836.*
19. Veraart J, Poot DH, Van Hecke W (2011) More accurate estimation of diffusion tensor parameters using diffusion Kurtosis imaging. *Magn Reson Med,* ***65(1):*** *138-145.*
20. Sridhar P, Mercier G, Tan J (2014) FDG PET metabolic tumor volume segmentation and pathologic volume of primary human solid tumors. *AJR Am J Roentgenol,* ***202(5):*** *1114-1119.*
21. Eisenhauer EA, Therasse P, Bogaerts J (2009) New response evaluation criteria in solid tumours: revised RECIST guideline (version 1.1). *Eur J Cancer,* ***45(2):*** *228-247.*
22. Moon SH, Choi JY, Lee HJ (2013) Prognostic value of 18F-FDG PET/CT in patients with squamous cell carcinoma of the tonsil: comparisons of volume-based metabolic parameters. *Head & neck,* ***35(1):*** *15-22.*
23. Pak K, Cheon GJ, Nam HY (2014) Prognostic value of metabolic tumor volume and total lesion glycolysis in head and neck cancer: a systematic review and meta-analysis. *J Nucl Med,* ***55(6):*** *884-890.*
24. Kim S, Oh S, Kim JS (2018) Prognostic value of FDG PET/CT during radiotherapy in head and neck cancer patients. *Radiat Oncol J,* ***36 (2):*** *95-102.*
25. Velasquez LM, Boellaard R, Kollia G (2009) Repeatability of 18F-FDG PET in a multicenter phase I study of patients with advanced gastrointestinal malignancies. *J Nucl Med,* ***50(10):*** *1646-1654.*
26. Westerterp M, Pruim J, Oyen W (2007) Quantification of FDG PET studies using standardised uptake values in multi-centre trials: effects of image reconstruction, resolution and ROI definition parameters. *Eur J Nucl Med Mol Imaging,* ***34(3):*** *392-404.*
27. Zhang Y, Liu X, Zhang Y (2015) Prognostic value of the primary lesion apparent diffusion coefficient (ADC) in nasopharyngeal carcinoma: a retrospective study of 541 cases. *Scientific reports,* ***5:*** *12242.*
28. Chen Y, Liu X, Zheng D (2014) Diffusion-weighted magnetic resonance imaging for early response assessment of chemoradiotherapy in patients with nasopharyngeal carcinoma. *Magn Reson Imaging,* ***32(6):*** *630-637.*
29. Basser PJ, Jones DK (2002) Diffusion-tensor MRI: theory, experimental design and data analysis - a technical review. *NMR Biomed,* ***15(7-8):*** *456-467.*
30. Lu H, Jensen JH, Ramani A (2006) Three-dimensional characterization of non-gaussian water diffusion in humans using diffusion kurtosis imaging. *NMR Biomed,* ***19(2):*** *236-247.*
31. Shima T, Fujima N, Yamano S (2020) Evaluation of non-Gaussian model-based diffusion-weighted imaging in oral squamous cell carcinoma: comparison with tumour functional information derived from positron-emission tomography. *Clin Radiol,* ***75(5):*** *397 e315-397 e321.*
32. Hori M, Fukunaga I, Masutani Y (2012) Visualizing non-Gaussian diffusion: clinical application of q-space imaging and diffusional kurtosis imaging of the brain and spine. *Magn Reson Med Sci,* ***11 (4):*** *221-233.*
33. Imaizumi A, Obata T, Kershaw J (2020) Imaging of Hypoxic Tumor: Correlation between Diffusion-weighted MR Imaging and (18)F-fluoroazomycin Arabinoside Positron Emission Tomography in Head and Neck Carcinoma. *Magn Reson Med Sci,* ***19(3):*** *276-281.*

[DOI: 10.61186/ijrr.22.3.603]